International Journal of Fracture, Vol. 16, No. 4, August 1980

Alphen aan den Rijn, The Netherlands

Interaction of antiplane shear waves by a Griffith crack at the interface of two bonded dissimilar elastic half-spaces

K.N. SRIVASTAVA, R.M. PALAIYA and D.S. KARAULIA

M.A. College of Technology, Bhopal (M.P.) India

(Received January 11, 1979; in revised form July 6, 1979)

ABSTRACT
The paper deals with the problem of finding the distribution of stress in the neighbourhood of a Griffith crack located at the interface of two bonded dissimilar elastic half-spaces. The crack is excited by a normally incident antiplane shear wave. The problem is reduced to that of solving a Fredholm integral equation. Both the iterative and numerical solutions have been obtained. The solutions are used for calculating numerical values of quantities of physical interest such as dynamic stress intensity factor and the amplitude of distance between the edges of the crack.

1. Introduction

The propagation of elastic waves in layered media has important applications in geophysics and siesmology. In spite of the fact that mathematically the problem is very cumbersome, a good amount of work has been done on this subject. An account of this work is available in two excellent monographs by Ewing et al. [1] and Brekovskikh [2]. A recent book on Elastodynamics by Eringen and Suhubi [3] contains a brief account of the propagation of P-, SV- and SH-waves in layered medium. The problem becomes still more complicated when an elastic wave propagating in a layered medium encounters a discontinuity at the interface of two layers having different elastic properties. The elastic wave undergoes reflection and refraction thus producing new waves. Thus we come across the phenomenon of diffraction of elastic waves in layered medium. The diffraction of waves certainly has important applications in seismology and oil technology. The study of dynamical fracture phenomenon, in spite of its great importance, is still at the stage of infancy.

Although the scattering of elastic waves by cracks located in homogeneous, isotropic, elastic solids has been the subject of many investigations, to our knowledge the diffraction of elastic waves with cracks located at the interface of two bonded elastic half-spaces has not been investigated so far. First attempt in this direction was made by Srivastava et al. [4, 5]. They have studied the interaction of longitudinal P-waves by a Griffith or a penny-shaped crack situated at the interface of two dissimilar elastic half-spaces bonded together. The scattered waves can be decomposed into a harmonic compressed wave (P-wave), vertically polarized wave (SV-wave) and horizontally polarized (SH-wave). The behaviour of SV-wave is similar to that of P-wave, it can be analysed by the method given in [4]. But the behaviour of SH-wave is somewhat different. Having discussed the behaviour of P-wave, it is natural to analyse the behaviour of SH-wave when it interacts with a line crack.

The purpose of this paper is to find the stress field in the neighbourhood of a Griffith crack located at the interface of two bonded dissimilar elastic half-spaces. The problem has been reduced to that of solving a Fredholm integral equation of the second kind. Both the iterative and numerical solutions of this integral equation have been obtained. These solutions are then used for calculating numerical values of dynamic stress intensity factor and the amplitude of the distance between the two edges of the crack for a wide range of frequencies. The results have been illustrated graphically. A comparison of these results has been made with those of Mal [6] and Sih and Loeber [7, 8] for homogeneous solid. The knowledge gained in this investigation is believed to be useful in understanding of the stress distribution in solids due to line cracks subjected to fluctuating loads.

2. Formulation of the problem

Let an open crack of infinite length and finite width be located at the interface of two bonded dissimilar elastic semi-infinite solids. Consider a rectangular cartesian coordinate system (x_1, x_2, x_3) at the center of the crack, so that the crack occupies the region $|x_1| \leq a$, $-\infty < x_2 < \infty$, $x_3 = 0$ at the interface of two half-spaces $x_3 > 0$ and $x_3 < 0$. The crack is assumed to be excited by a normally incident antiplane shear wave originating at $x_3 = -\infty$. The displacement vector corresponding to this wave is parallel to x_2-axis. It is convenient to make all the quantities dimensionless by writing $x_1/a = x$, $x_2/a = y$, $x_3/a = z$.

Thus we have the problem of finding stress distribution when the crack is subjected to the following boundary conditions

$$\sigma_{yz}(x, 0+) = \sigma_{yz}(x, 0-) = -p_s - p_0 \exp(-i\omega t), \quad |x| \leq 1 \tag{2.1}$$

$$\sigma_{yz}(x, 0+) = \sigma_{yz}(x, 0-), \quad |x| > 1 \tag{2.2}$$

$$u_y(x, 0+) = u_y(x, 0-) \quad |x| > 1 \tag{2.3}$$

where ω is the circular frequency and p_s is the static pressure which is assumed to be sufficiently large so that the crack faces do not come in contact during vibration. In the latter part of the discussion the time factor $\exp(-i\omega t)$ will be omitted but understood. The problem of finding stress distribution reduces to that of obtaining the solution of the displacement equation

$$u_{y,xx} + u_{y,zz} + k^2 u_y = 0, \tag{2.4}$$

where $k^2 = (a\omega)^2\rho/\mu$, μ is Lame's constant and ρ is the material density. The solution of this equation is:

$$u_y(x, z) = \begin{cases} \int_0^\infty A_1(\xi) \exp(-\beta_1 z) \cos \xi x \, d\xi, & z > 0 \\ \int_0^\infty A_2(\xi) \exp(\beta_2 z) \cos \xi x \, d\xi, & z < 0, \end{cases} \tag{2.5}$$

where

$$\begin{aligned} \beta_i &= \begin{cases} (\xi^2 - k_i^2)^{1/2}, & k_i < \xi, \\ -i(k_i^2 - \xi^2)^{1/2}, & k_i > \xi, \end{cases} \\ k_i^2 &= (a\omega)^2\rho_i/\mu_i, \qquad i = 1, 2. \end{aligned} \tag{2.6}$$

The suffixes 1 and 2 correspond to the half-spaces $z > 0$ and $z < 0$ respectively. In Eqn. (2.5) $A_1(\xi)$ and $A_2(\xi)$ are unknown functions which will be determined with the help of the boundary conditions. The corresponding expression for stress components are

$$\sigma_{yz}(x, z) = \begin{cases} -2\mu_1 \int_0^\infty \beta_1 A_1(\xi) \exp(-\beta_1 z) \cos \xi x \, d\xi, & z > 0, \\ 2\mu_2 \int_0^\infty \beta_2 A_2(\xi) \exp(\beta_2 z) \cos \xi x \, d\xi, & z > 0, \end{cases} \tag{2.7}$$

3. Derivation of the integral equation

From conditions (2.1) and (2.2) we see that $\sigma_{yz}(x, 0+) = \sigma_{yz}(x, 0-)$ for all values of x, hence we have

$$A_2(\xi) = -\frac{\mu_1\beta_1}{\mu_2\beta_2} A_1(\xi). \tag{3.1}$$

The boundary conditions (2.1) and (2.3) lead to the following dual integral equations

$$\int_0^\infty \beta_1 A_1(\xi) \cos \xi x \, d\xi = p_0/2\mu_1, \qquad |x| < 1, \tag{3.2a}$$

$$\int_0^\infty \frac{\mu_1\beta_1 + \mu_2\beta_2}{\beta_2} A_1(\xi) \cos \xi x \, d\xi = 0, \quad |x| > 1, \tag{3.2b}$$

It is convenient to write

$$\left(\frac{\mu_1\beta_1 + \mu_2\beta_2}{\beta_2}\right) A(\xi) = B(\xi) \tag{3.3}$$

With this substitution the above integral equations become

$$\int_0^\infty \xi[1 + H(\xi)]B(\xi) \cos \xi x \, d\xi = \frac{\mu_1 + \mu_2}{2\mu_1} p_0, \quad |x| < 1 \tag{3.4}$$

$$\int_0^\infty B(\xi) \cos \xi x \, d\xi = 0, \quad |x| > 1 \tag{3.5}$$

where $H(\xi) = \dfrac{(\mu_1 + \mu_2)\beta_1\beta_2}{(\mu_1\beta_1 + \mu_2\beta_2)} - 1$ (3.6)

Let the trail solution of the above system of dual integral equations be:

$$B(\xi) = \frac{p_0(\mu_1 + \mu_2)}{2\mu_1} \int_0^1 tg(t)J_0(\xi t) \, dt \tag{3.7}$$

The Eqn. (3.5) is satisfied and from (3.4) we get the following Fredholm integral equation of the second kind for determining the unknown function $g(t)$.

$$g(u) + \int_0^1 tg(t)L(u, t) \, dt = 1 \tag{3.8}$$

where $L(u, t) = \displaystyle\int_0^\infty \xi H(\xi)J_0(\xi u)J_0(\xi t) \, d\xi$ (3.9)

For homogeneous medium the above integral equation reduces to the integral equation obtained by Mal [6]. The integrand in (3.9) has no poles, it has only branch points at $\xi = k_1$ $\xi = k_2$. The infinite integral in Eqn. (3.9) can be converted into integrals with finite limits by the procedure given in [6]. Let

$$I = \int_{k_1}^\infty M(\xi, \beta_2, \beta_1)J_0(\xi u)J_0(\xi t) \, d\xi \tag{3.10}$$

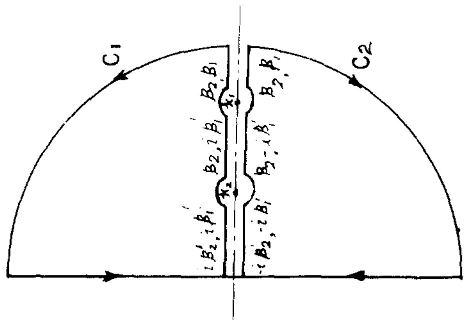

Figure 1. The contours of integration for the integrals in (3.12) and (3.13).

where $M(\xi, \beta_2, \beta_1) = H(\xi)$ (3.11)

Consider the integrals

$$I_1 = \oint_{C_1} M(\xi, \beta_2, \beta_1) J_0(\xi u) H_0^{(1)}(\xi t)\, \mathrm{d}\xi \tag{3.12}$$

$$I_2 = \oint_{C_2} M(\xi, \beta_2, \beta_1) J_0(\xi u) H_0^{(2)}(\xi t)\, \mathrm{d}\xi. \tag{3.13}$$

The contour C_1 and C_2 are defined in Fig. 1. Since the integrands in (3.12) and (3.13) satisfy Jordan's Lemma on the infinite quarter circles, hence we have

$$\begin{aligned} I = &-\tfrac{1}{2} \int_0^{k_2} \xi J_0(\xi u)[M(\xi, \mathrm{i}\beta_2', \mathrm{i}\beta_1') H_0^{(1)}(\xi t) + M(\xi, -\mathrm{i}\beta_2', -\mathrm{i}\beta_1') H_0^{(2)}(\xi t)]\mathrm{d}\xi \\ &-\tfrac{1}{2} \int_{k_2}^{k_1} \xi J_0(\xi u)[M(\xi, \beta_2', +\mathrm{i}\beta_1') H_0^{(1)}(\xi t) + M(\xi, \beta_2', -\mathrm{i}\beta_1') H_0^{(2)}(\xi t)]\, \mathrm{d}\xi \end{aligned} \tag{3.14}$$

where $\beta_j' = (k_j^2 - \xi^2)^{1/2}, \quad j = 1, 2.$

Substituting the value of $M(\xi, \beta_2, \beta_1)$ and afer using (3.14) in (3.10) we get

$$\begin{aligned} L(u, t) = &-\mathrm{i}(\mu_1 + \mu_2) k_1^2 \int_0^{\gamma} \frac{J_0(\xi k_1 u) H_0^{(1)}(\xi k_1 t)(\gamma^2 - \xi^2)^{1/2}(1 - \xi^2)^{1/2}}{\mu_1(1 - \xi^2)^{1/2} + \mu_2(\gamma^2 - \xi^2)^{1/2}}\, \mathrm{d}\xi \\ &-\mathrm{i}\mu_2(\mu_1 + \mu_2) k_1^2 \int_{\gamma}^{1} \frac{J_0(\xi k_1 u) H_0^{(1)}(\xi k_1 t)(\xi^2 - \gamma^2)(1 - \xi^2)^{1/2}}{\mu_1^2(1 - \xi^2) + \mu_2^2(\xi^2 - \gamma^2)}\, \mathrm{d}\xi \end{aligned} \tag{3.15}$$

where $\gamma = (k_2/k_1) < 1$. In case when $k_2/k_1 > 1$, let $\gamma_1 = k_1/k_2 < 1$. By interchaning the positions of k_1, β_1, β_1' and k_2, β_2, β_2' in the above contours we get

$$\begin{aligned} L(u, t) = &-\mathrm{i}(\mu_1 + \mu_2) k_2^2 \int_0^{\gamma_1} \frac{J_0(\xi k_2 u) H_0^{(1)}(\xi k_2 t)(\gamma_1^2 - \xi^2)^{1/2}(1 - \xi^2)^{1/2}}{\mu_1(\gamma_1^2 - \xi^2)^{1/2} + \mu_2(1 - \xi^2)^{1/2}}\, \mathrm{d}\xi \\ &-\mathrm{i}\mu_1(\mu_1 + \mu_2) k_2^2 \int_{\gamma_1}^{1} \frac{J_0(\xi k_2 u) H_0^{(1)}(\xi k_2 t)(\xi^2 - \gamma_1^2)(1 - \xi^2)^{1/2}}{\mu_1^2(\xi^2 - \gamma_1^2) + \mu_2^2(1 - \xi^2)}\, \mathrm{d}\xi. \end{aligned} \tag{3.16}$$

4. Quantities of physical interest

The singular part of the stress component in the neighbourhood of the crack tip can be obtained by using Eqns. (2.7), (3.3) and (3.7). Hence, for $|x| > 1$, we have

$$\sigma_{yz}(x, 0+) = \sigma_{yz}(x, 0-) = \frac{p_0 x}{(x^2 - 1)^{1/2}} g(1) + 0(1) \tag{4.1}$$

Dynamic stress intensity factor is defined by the relation

$$N_z = \lim_{x \to 1+} (x-1)^{1/2} |\sigma_{yz}(x, 0+)| \tag{4.2}$$

Hence we get

$$N_z = \frac{p_0}{\sqrt{2}} |g(1)| \tag{4.3}$$

In elastostatic case the stress intensity factor is $N_z^0 = p_0/\sqrt{2}$. Thus we have

$$N_z/N_z^0 = |g(1)|. \tag{4.4}$$

Another quantity of physical interest is the amplitude of the distance between the two edges of the crack. From Eqns. (2.5), (3.3) and (3.7) for $0 \leq |x| \leq 1$, we have

$$\begin{aligned} D(x) = |u_y(x, 0+) - u_y(x, 0-)| &= \frac{p_0(\mu_1+\mu_2)}{2\mu_1\mu_2} \left| \int_x^1 \frac{tg(t)}{(t^2-x^2)^{1/2}} \, dt \right| \\ &= p_0 \frac{(\mu_1+\mu_2)}{2\mu_1\mu_2} \left| (1-x^2)^{1/2} g(1) - \int_x^1 (t^2-x^2)^{1/2} g'(t) \, dt \right| \end{aligned} \tag{4.5}$$

For the static case the value of the distance between the two edges of the crack at the center of the crack is

$$D_0 = p_0 \frac{(\mu_1+\mu_2)}{2\mu_1\mu_2}.$$

Normalizing $D(x)$ with respect to the static displacement between the two edges of the crack at the center, we get

$$D = D(x)/D_0 = \left| (1-x^2)^{1/2} g(1) - \int_x^1 (t^2-x^2)^{1/2} g'(t) \, dt \right| \tag{4.6}$$

The dynamic crack energy is given by the relation

$$\begin{aligned} W &= 2 \left| \int_0^1 p_0 \{u_y(x, 0+) - u_y(x, 0-)\} \, dx \right| \\ &= \frac{p_0^2(\mu_1+\mu_2)\pi}{2\mu_1\mu_2} \left| \int_0^1 tg(t) \, dt \right|. \end{aligned} \tag{4.7}$$

For elastostatic case

$$W_0 = \frac{p_0^2(\mu_1+\mu_2)\pi}{4\mu_1\mu_2}. \tag{4.8}$$

Hence we have

$$W/W_0 = 2 \left| \int_0^1 tg(t) \, dt \right|. \tag{4.9}$$

5. Solution of the integral equation

In this section, we shall obtain both the iterative and numerical solutions of the integral equation (3.8). The iterative solution is valid for small values of k_1 and k_2. The numerical solution has been obtained for a wide range of frequencies.

For small values of the argument the Bessel functions $J_0(x)$ and $H_0^{(1)}(x)$ may be expanded in ascending powers of x as

$$J_0(x) = \sum_{n=0}^{\infty} a_{2n} x^{2n}, \quad H_0^{(1)}(x) = \left[1 + \frac{2i}{\pi} \log \frac{x}{2}\right] J_0(x) + i \sum_{n=0}^{\infty} b_{2n} x^{2n}$$

where $a_0 = 1$ and the values of other coefficients a_{2n} and b_{2n} are given in [9, p. 369]. Using the above expression in (3.15), $L(u, t)$ can be expressed as

$$L(u, t) = (k_1^2 \log k_1)L_1(u, t) + k_1^2 L_2(u, t) + (k_1^2 \log k_1)^2 L_3(u, t) + (k_1^4 \log k_1)L_4(u, t) + o(k_1^4) \tag{5.1}$$

where

$$L_1(u, t) = \frac{2M_0}{\pi}, \quad L_2(u, t) = \frac{2N_0}{\pi} + \left(b_0 i - i + \frac{2}{\pi}\log\frac{t}{2}\right)M_0$$

$$L_3(u, t) = 0, \quad L_4(u, t) = \frac{2a_2N_2}{\pi}(u^2 + t^2), \quad u < t,$$

$$M_{2n} = \int_0^\gamma \alpha(\xi)\,\mathrm{d}\xi + \int_\gamma^1 \beta(\xi)\,\mathrm{d}\xi$$

$$N_{2n} = \int_0^\gamma \alpha(\xi)\log\xi\,\mathrm{d}\xi + \int_\gamma^1 \beta(\xi)\log\xi\,\mathrm{d}\xi, \quad n = 0, 1, 2, \ldots$$

$$\alpha(\xi) = (\mu_1 + \mu_2)\frac{\xi^{2n}(\gamma^2 - \xi^2)^{1/2}(1 - \xi^2)^{1/2}}{\mu_1(1 - \xi^2)^{1/2} + \mu_2(\gamma^2 - \xi^2)^{1/2}}$$

$$\beta(\xi) = \mu_2(\mu_1 + \mu_2)\frac{\xi^{2n}(\xi^2 - \gamma^2)(1 - \xi^2)^{1/2}}{\mu_1^2(1 - \xi^2) + \mu_2^2(\xi^2 - \gamma^2)}.$$

Assuming that $g(u)$ can be expanded in the form

$$g(u) = g_0(u) + k_1^2 \log k_1 g(u) + k_1^2 g_2(u) + (k_1^2 \log k_1)^2 g_3(u) + k_1^4 \log k_1 g_4(u) + 0(k_1^4) \tag{5.2}$$

and substituting in (3.8), the following iterative scheme is obtained

$$g_0(u) = 1, \quad g_1(u) = -\int_0^1 tL_1(u, t)\,\mathrm{d}t = -\frac{M_0}{\pi}$$

$$g_2(u) = -\int_0^1 tL_2(u, t)\,\mathrm{d}t = -\frac{N_0}{\pi} - \frac{M_0}{2}\left(ib_0 - i + \frac{2}{\pi}\log\tfrac{1}{2}\right) + (1 - u^2)\frac{M_0}{2\pi}$$

$$g_3(u) = -\int_0^1 t[L_1(u, t)g_1(t) + L_3(u, t)]\,\mathrm{d}t = (M_0/\pi)^2$$

$$g_4(u) = -\int_0^1 t[L_1(u, t)g_2(t) + L_2(u, t)g_1(t) + L_4(u, t)]\,\mathrm{d}t$$
$$= \frac{M_0}{\pi}\left\{\frac{2N_0}{\pi} + M_0\left(ib_0 - i + \frac{2}{\pi}\log\tfrac{1}{2}\right)\right\} + (1 + 2u^2)\frac{a_2N_2}{2\pi} - (3 - 2u^2)\left(\frac{M_0}{2\pi}\right)^2.$$

The above iterative solution is valid for $k_2/k_1 < 1$ and for small values of k_1. When $\gamma_1 = k_1/k_2 < 1$ and k_2 is small the iterative solution is

$$g(u) = g_0(u) + k_2^2 \log k_2 g_1(u) + k_2^2 g_2(u) + (k_2^2 \log k_2)^2 g_3(u) + k_2^4 \log k_2 g_4(u) + 0(k_2^4) \tag{5.3}$$

where $g_n(u)$ have the above values with

$$M_{2n} = \int_0^{\gamma_1} \alpha_1(\xi)\,\mathrm{d}\xi + \int_{\gamma_1}^1 \beta_1(\xi)\,\mathrm{d}\xi$$

$$N_{2n} = \int_0^{\gamma_1} \alpha_1(\xi)\log\xi\,\mathrm{d}\xi + \int_{\gamma_1}^1 \beta_1(\xi)\log\xi\,\mathrm{d}\xi$$

$$\alpha_1(\xi) = (\mu_1 + \mu_2)\frac{\xi^{2n}(\gamma_1^2 - \xi^2)^{1/2}(1-\xi^2)^{1/2}}{\mu_1(\gamma_1^2 - \xi^2)^{1/2} + \mu_2(1-\xi^2)^{1/2}}$$

$$\text{and } \beta_1(\xi) = \mu_1(\mu_1 + \mu_2)\frac{\xi^{2n}(\xi^2 - \gamma_1^2)(1-\xi^2)^{1/2}}{\mu_1^2(\xi^2 - \gamma_1^2) + \mu_2^2(1-\xi^2)}$$

The integral equation (3.8) has been solved numerically for a wide range of frequencies. The solution has been obtained for the following two sets of materials. First set:

Aluminium	$\rho_1 = 2.7\ \text{gm/cm}^3$,	$\mu_1 = 2.63 \times 10^{11}\ \text{dyne/cm}^2$
Steel	$\rho_2 = 7.6\ \text{gm/cm}^3$,	$\mu_2 = 8.32 \times 10^{11}\ \text{dyne/cm}^2$

Second set:

Wrought iron	$\rho_1 = 7.8\ \text{gm/cm}^3$,	$\mu_1 = 7.7 \times 10^{11}\ \text{dyne/cm}^2$
Copper	$\rho_2 = 8.96\ \text{gm/cm}^3$,	$\mu_2 = 4.5 \times 10^{11}\ \text{dyne/cm}^2$.

With the help of Fox and Goodwin's method [10], the integral equations was converted into a system of linear algebraic equations. For this purpose the values of the kernel function $L(u, t)$ were evaluated by using Simpson's quadrature formula. For the first pair of material $k_2/k_1 < 1$, hence the values of $L(u, t)$ were computed from (3.15). While for the second set of materials $\gamma_1 = k_1/k_2 < 1$, hence (3.16) was used for computing the values of $L(u, t)$. At relatively high frequencies, the number of divisions in the interval (0, 1) wre increased until the solution of the integral equation reaches a stable value. A complex computer programming was used for obtaining the values of $g(u)$. These values were used for calculating numerical values of dynamic stress intensity factor from (4.3).

The amplitude of $|g(1)|$ has been plotted against k_1 in Fig. 2. In this figure the continuous curve represents the values of $|g(1)|$ obtained from numerical calculations while the dotted curve represents the values obtained from the iterative solution. Since the two curves overlap for values of $k_1 < 0.6$, we conclude that the five term iterative solution given by (5.2) quite accurately predicts the behaviour of the interaction phenomena in the range $0 < k_1 < 0.6$. Mal [11] has obtained a similar result for homogeneous solids. The accuracy of the approximate solution can be improved by including more terms in the series solution. However, for the majority of elastic materials, the shear wave velocity is greater than 2×10^5 cm/sec. If the crack length is assumed to be of the order 10^{-4} cm, the circular frequency ω can be as high as 10^9

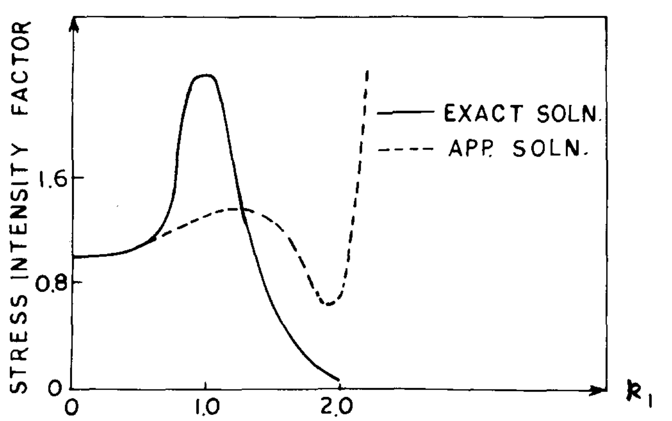

Figure 2. Amplitude of $|g(1)|$ plotted against frequency.

cycles/sec, even then we have $k_1 < 0.6$. Thus in most practical cases the approximate analytical solution given in (5.2) is sufficiently accurate to predict the behaviour of the crack under dynamic loading. It is interesting to note that Mal [11] has arrived at a similar conclusion for homogeneous solids.

Next we shall compare our results with those of Mal [6] and Sih and Loeber [7] for homogeneous solids. Sih and Loeber have studied the problem for low frequencies while Mal has studied the problem for a wide range of frequencies. For low frequencies their results are in good agreement. Hence we shall compare our results with those of Mal. With this object in view, we have plotted the amplitude of stress intensity factor against frequency on the same scale as that of Mal [6] in Fig. 3. The continuous curve is for $k_2/k_1 < 1$, while the broken line curve is for the case $k_1/k_2 < 1$. Mal's results are shown by the dotted curve. In contrast to a homogeneous medium, for bonded solids the stress intensity factor increases at first slowly up to $k_1 = 0.5$, then it rises suddenly reaching a first maxima at $k_1 = 0.98$. The dynamic stress intensity factors in both the bonded and homogeneous solids exceed the corresponding static value, but for bonded solids this increase is much greater than that for homogeneous solids. Another interesting feature is that both in the homogeneous as well as in the bonded solids the stress intensity factors drop rapidly beyond the first maxima and exhibit oscillations of approximately constant period as the frequency increases. But the decay in the amplitude in bonded solids is greater than that in homogeneous medium. Moreover the period of oscillations at higher frequencies in bonded medium is greater when compared with homogeneous medium.

The amplitude of the normalized distance between the two edges of a crack given by (4.6) are plotted for several values of k_1 and at different points along the crack in Fig. 4 (a) and Fig. 4 (b). The results show that the amplitude increases until the frequencies reach the values that correspond to the first maxima in Fig. 3. But in contrast to homogeneous medium, in bonded medium even for relatively low frequencies, the curves greatly differ from those for the static case. In bonded medium even at low freqeuncies, oscillations are introduced as a result of the interference of waves inside the crack. At higher frequencies our curves exhibit the same characteristics as those obtained by Mal [6] for homogeneous medium, with the only difference being that the amplitude of displacement decreases as frequency increases.

The amplitudes of normalized crack energy given by (4.7) are plotted against k_1 in

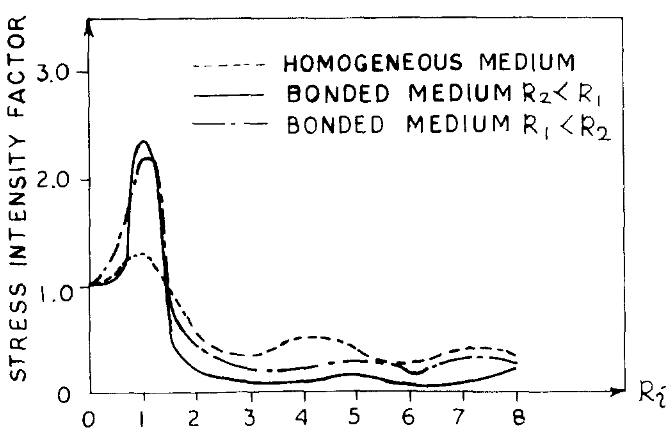

Figure 3. Amplitude of $|g(1)|$ plotted against frequency. For $R_2 < R_1$, $R_i = R_1$ and for $R_1 < R_2$, $R_i = R_2$.

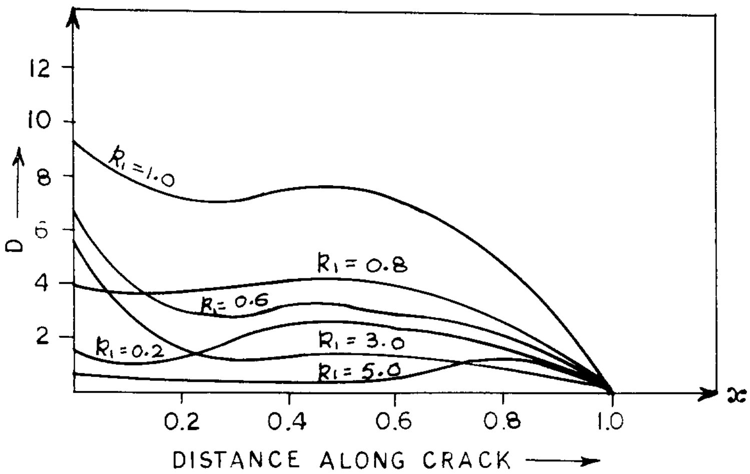

Figure 4 (a). D: Amplitude of the distance between the two faces of the crack. Normalized with respect to the distance for the static case at the center of the crack.

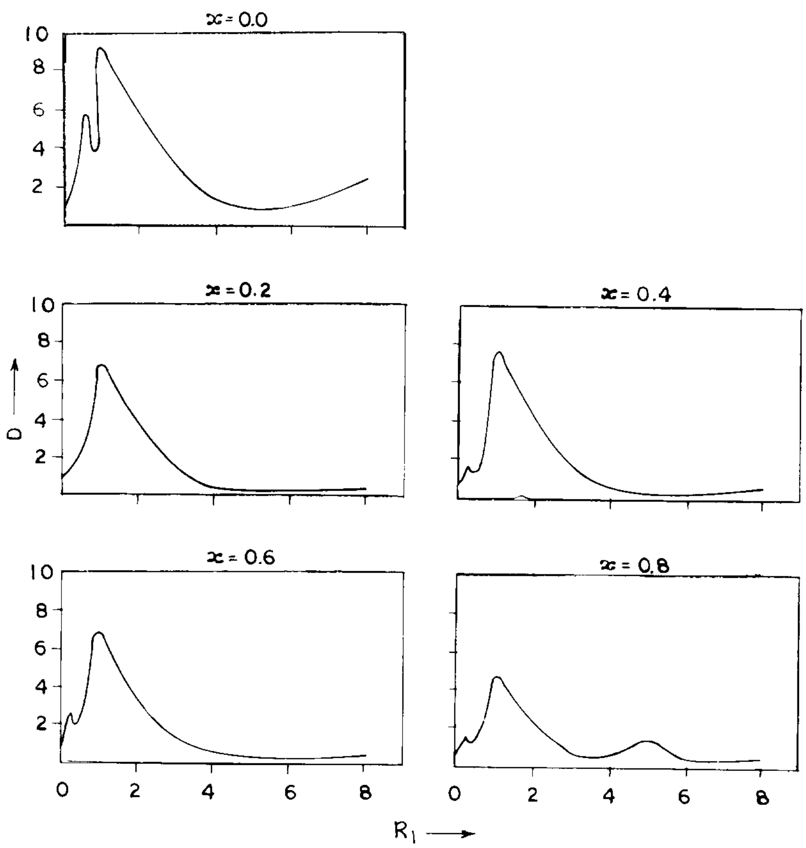

Figure 4 (b). The amplitude of D plotted against R_1 at different points along the crack.

Fig. 5. The results show that a first maxima occurs at relatively low frequency but the second maxima corresponds to the first maxima in the curves in Fig. 3, after this maxima the crack energy drops rapidly and exhibits oscillations as frequency increases.

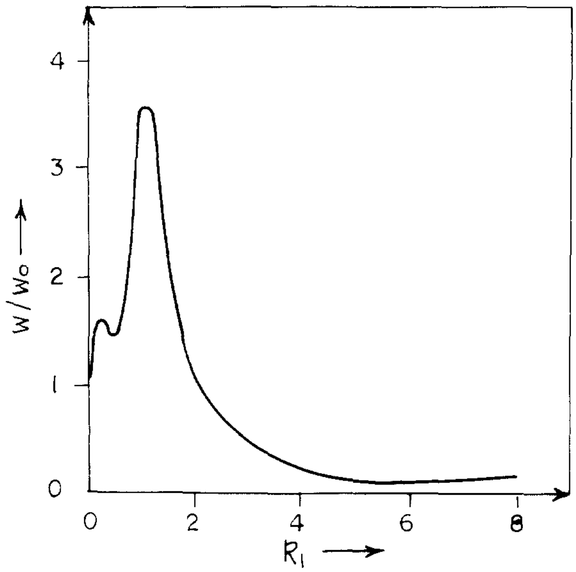

Figure 5. Energy plotted against R_1.

Acknowledgments

The authors are grateful to the referees for their valuable comments which were quite useful in revising the paper.

This research was supported by U.G.S grant No. F. 23-88/75.

REFERENCES

[1] W.M. Ewing, W.S. Jardetsky and F. Press, Elastic waves in layered media., McGraw-Hill, New York (1957).

[2] L.M. Brekhovskikh, Waves in layered media., Izat. Akad. Nauk. SSSR Maskov (1957) English translation. Academic Press, New York (1960).

[3] A.C. Eringen and E.S. Suhubi, Elastodynamics. Vol. II Linear theory. Academic Press (1975).

[4] K.N. Srivastava, R.M. Palaiya and O.P. Gupta, *International Journal of Fracture*, 14 (1978) 145–154.

[5] K.N. Srivastava, R.M. Palaiya and O.P. Gupta, *International Journal of Fracture*, 15 (1979) 591–599.

[6] A.K. Mal, *International Journal of Engineering Science*, 8 (1970) 763.

[7] G.C. Sih and J.F. Loeber, *Quarterly of Applied Mathematics*, 27 (1969) 193.

[8] J.F. Loeber and G.C. Sih, *Journal of the Acoustical Society of America*, 44 (1968) 90.

[9] M. Abramowitz and I.A. Stegun, Handbook of Mathematical Functions. Dover, New York (1965).

[10] L. Fox and E.T. Goodwin, Philosophical Transactions of the Royal Society, A 245 (1953) 501.

[11] A.K. Mal, *International Journal of Engineering Science*, 10 (1972) 609.

RÉSUMÉ

Le mémoire est relatif au problème qui consiste à trouver la distribution des contraintes au voisinage d'une fissure de Griffith située à l'interface de deux demi-espaces élastiques dissemblables et collés. La fissure est mise en mouvement par une onde de cisaillement antiplanaire avec une incidence normale. Le problème est ramené à celui de trouver une équation intégrale de Fredholm. On a obtenu à la fois des solutions itératives et numériques. Ces solutions sont utilisées pour calculer les valeurs numériques de certaines quantités d'intérêt physique, telles que le facteur d'intensité des contraintes dynamiques, et l'étendue de la distance entre les extrémités d'une fissure.